• **The Formation of the First Luminous Sources** The reionization of the Universe imprints multiple signals in the temperature and polarization of the CMB. In polarization, the most important signal is an enhancement in the EE power spectrum at large angular scales $\ell \lesssim 20$; see Figure **??**. This signal gives a direct measurement of the optical depth to the reionization epoch τ, and thus to the mean redshift of reionization z_{re}, with very little degeneracy with other cosmological parameters; see Figure **??**. The mean redshift of reionization z_{re} (when 50% of the cosmic volume was reionized) depends sensitively on the nature of the ionizing sources. It is currently unknown whether star-forming galaxies or more exotic sources such as supermassive black holes drove the reionization process. What was the mean free path of ionizing photons during this epoch? What was the efficiency with which such photons were produced by ionizing sources? What were the masses and environments of the dark matter halos that hosted the sources? These properties all affect z_{re}. Furthermore, the detailed shape of the low-ℓ E-mode power spectrum is sensitive to the reionization history itself (i.e., $d\tau/dz$), and will provide information beyond that captured in τ alone. For example, it has been argued that *Planck* data show evidence for an extended tail of reionization out to $z \approx$ 15-20 (**?**). A cosmic-variance-limited measurement of the large-scale E modes, as obtained by PICO, will settle this question.

Large-scale EE power spectrum measurements are a unique and crucial observable for many aspects of cosmology, particularly the growth of structure. If measurements of τ are not improved beyond the current uncertainties from *Planck*, inference of several new signals of cosmological physics will be severely hindered. A canonical example is the inference of the sum of the neutrino mass (see page **??** but any cosmological inference related to the growth of structure will be affected to some extent, including constraints on dark energy and modified gravity from weak lensing, cluster counts, and other structure probes. PICO is the ideal experiment to resolve this issue. Its noise level and frequency coverage permit a cosmic-variance-limited constraint on τ, i.e., $\sigma(\tau) \approx 0.002$, which we have verified with explicit forecasts including separation of foregrounds.

In temperature, the most important imprint of reionization is that sourced at small angular scales by the "patchy" kinematic Sunyaev-Zel'dovich (kSZ) effect, due to the peculiar velocities of free electron bubbles around ionizing sources. It is possible to extract reionization constraints from the small-scale kSZ power spectrum (**?**). The most directly constrained quantity is the duration of reionization, Δz_{re}.

Fig. **??** presents forecasts for reionization constraints in the z_{re}-Δz_{re} parameter space obtained from PICO's measurement of τ in combination with ground-based Stage-III (CMB-S3) constraints on the kSZ power spectrum. Constraints from existing *Planck* data and observations at other wavelengths are also presented. The PICO measurement of τ is essential for breaking degeneracies (compare the dashed and solid contours) and allowing simultaneous, precise constraints to be placed on both the mean redshift and duration of reionization. Fig. **??** also shows curves of constant source efficiency (i.e., the efficiency of ionizing photon production) and constant intergalactic medium opacity (i.e., the photon mean free path). PICO will allow simultaneous constraints to be placed on these physical parameters, yielding important information on the nature of the first luminous sources (e.g., star-forming galaxies or quasars predict significantly different values for these parameters).

In addition to these signals, reionization also leaves specific non-Gaussian signatures in the CMB. In particular, patchy reionization induces non-trivial 4-point functions in both temperature (**?**) and polarization (**?**). The temperature 4-point function can be used to separate reionization and late-time kSZ contributions. Combinations of temperature and polarization data can be used to build quadratic estimators for reconstruction of the patchy τ field, analogous to CMB lensing recon-

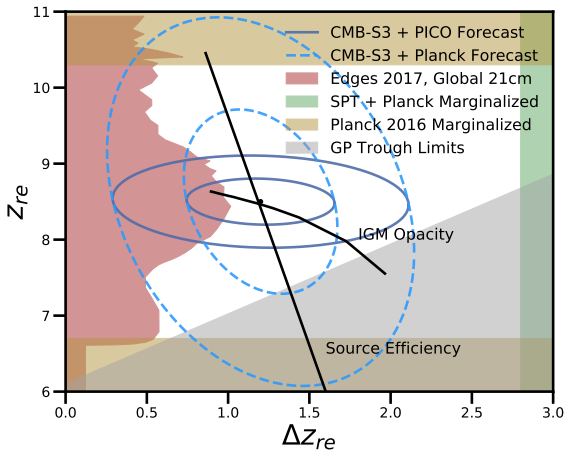

Figure 1: Summary of constraints on the mean redshift and duration of reionization. The forecasts show 68% and 95% confidence-level contours for PICO combined with CMB-S3 experiments and Planck combined with CMB-S3 experiments (dark blue and dashed blue, respectively). The solid black lines illustrate how the IGM opacity and source efficiency model parameters map onto this parameter space. The forecasted PICO constraints are compared to: current exclusion limits for the mean redshift of reionization from Planck, shown by the yellow bands **?**; recent exclusion limits from the global 21 cm signal measured by EDGES, shown with the red band **?**; exclusion limits from measurements of the Gunn-Peterson trough from fully absorbed Lymanα in quasar spectra, shown by the grey band **?**; exclusion limit on the duration of reionization from Planck and SPT data, shown by the green band **?**.

struction. These estimators generally require high angular resolution, but also rely on foreground-cleaned CMB maps. Thus, while PICO alone may not enable high S/N reconstructions, its high-frequency channels — which have better than 2 arcmin resolution and observe at frequencies that have yet to be demonstrated from the ground — will enable these estimators to be robustly applied to ground-based CMB data sets, a strong example of ground-space complementarity.

• **Structure Formation via Gravitational Lensing** Matter between us and the last-scattering surface deflects the path of photons through gravitational lensing, imprinting the 3-dimensional matter distribution across the volume of the universe onto the CMB maps. The specific quantity being mapped by the data is the projected gravitational potential ϕ that is lensing the photons. From the lensing map, which receives contributions from all redshifts between us and the CMB with the peak of the distribution at $z \simeq 2$, we infer the angular power spectrum $C_L^{\phi\phi}$. Both the temperature and polarization maps of the CMB, and by extension the angular power spectra, are affected by lensing.

Planck's ϕ map had **SNR!** (**SNR!**) of $\sim$1 per L mode over a narrow range of scales, $30 < L < 50$. PICO's map would represents true mapping, with **SNR!** $>>$ 1 per each mode down to scales of approximately ten arcminutes ($L \sim 1000$); see Figure **??**. On smaller scales, the map will still contain statistical information. While *Planck* had an **SNR!** of 40 integrated across the $C_L^{\phi\phi}$ power spectrum (**?**), the PICO combination of resolution, sensitivity, and sky coverage enables a measurement with SNR of 638 and 737 for the baseline and CBE configurations, respectively. When accounting for possible foreground contamination, its broad frequency coverage leads to a reduction of SNR of less than 20%; see Figure **??**.

The value of the reconstructed lensing map is immense, as has already been demonstrated with the much lower **SNR!** map from *Planck*. The unprecedented constraints on neutrino mass, discussed in page **??**, are a direct result of this deep map. Tomographic cross-correlations of the lensing map with samples of galaxies and quasars will yield constraints on structure formation. The measurements will constrain the properties of quasars and other high-redshift astrophysics, e.g., a precise determination of the quasar bias (and hence host halo mass) as a function of their properties, such as (non-)obscuration. The map will be cross-correlated with other large scale tracers to probe fun-

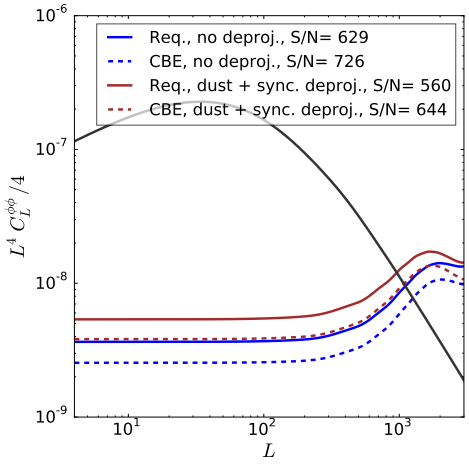

Figure 2: The theoretically predicted lensing power spectrum $C_L^{\phi\phi}$ (black) and forecasted PICO noise levels, with (red), and without (blue) deprojection, that is removal, of foregrounds. PICO will make a map of ϕ at angular scales where the noise is below the signal.

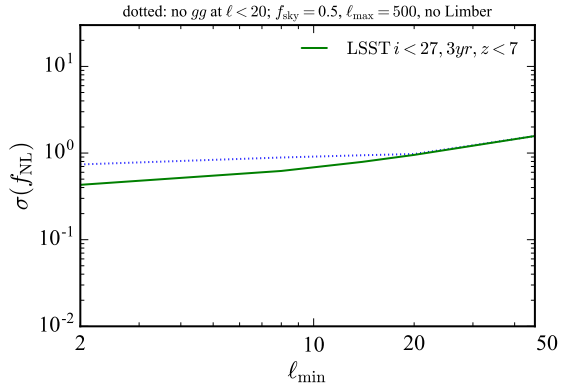

Figure 3: Forecasted sensitivity to the parameter describing primordial non-Gaussianity of the local type for the PICO CMB lensing map together with three years of the LSST survey, as a function of the minimal multipole used in the analysis. A value of $\sigma(f_{\rm NL}) \simeq 1$ is a well-motivated theoretical target.

damental physics. For instance, one can use correlations between large scale structure tracers with different clustering bias factors to effectively cancel cosmic variance (**??**) and constrain physics that affects the biasing of objects on large scales, such as primordial local non-Gaussianity (**?**). In Fig. **??** we show the expected constraints for the CMB lensing field as reconstructed with PICO, in cross correlation with three years of the LSST survey. It can be seen that depending on the minimal multipole that can be used in the cross correlation, which is uncertain in both LSST and the PICO lensing map, the well-motivated theory target of $\sigma(f_{\rm NL}) \simeq 1$ (**?**) can be within reach. Values of $f_{\rm NL}$ at or above this level are a generic prediction of multi-field inflationary models.

Using the same cross-correlation techniques, it is also possible to constrain the evolution of the amplitude of structure as a function of redshift. Figure **??** shows constraints on the amplitude of linear structure in several redshift bins. This is a model-independent representation of the structure growth constraints; these measurements will yield constraints on dark energy or modified gravity, in the context of specific models. The measurements can also be used for a neutrino mass constraint that is complementary to and competitive with that inferred from the CMB lensing auto-power spectrum described earlier.

Lensing will also be used to weigh dark matter halos hosting galaxies, groups, and clusters of galaxies. Calibrating the masses of galaxy clusters is the most uncertain and crucial step in the cluster cosmology program, in which CMB lensing has already begun to play an important role. In this approach, known as CMB halo lensing, we focus on the small-scale effects of gravitational lensing around these objects (**???**). The technique holds great potential for measuring halo masses out to high redshifts where gravitational lensing of galaxies (i.e., gravitational shear) no longer works because of the lack of background sources.

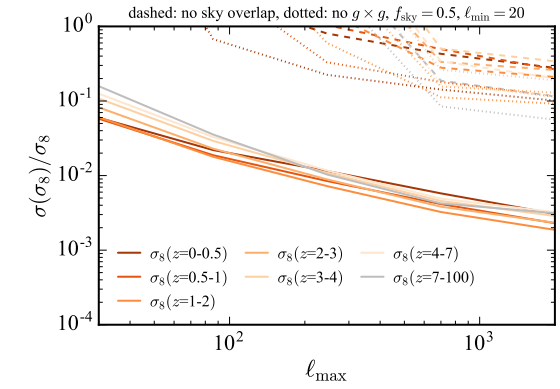

Figure 4: Forecasted sensitivity to the parameter describing the amplitude of structure in various redshift bins, as a function of the maximal multipole used in the analysis. Percent-level constraints on these parameters allow for stringent tests of physics beyond ΛCDM that modify the rate of growth of structure.

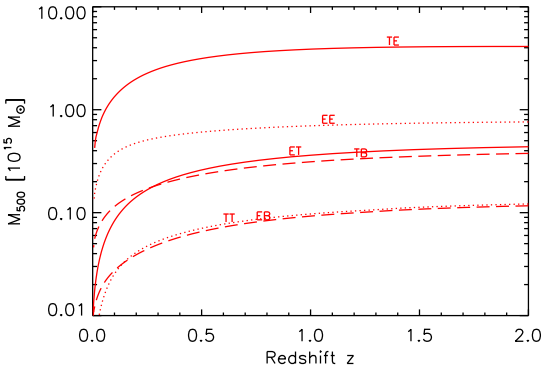

Figure 5: PICO sensitivity for CMB halo lensing. The different curves give the one-sigma sensitivity of an optimal mass filter (**?**) using different possible lensing estimators constructed from both temperature and polarization anisotropy measurements. The curves are flat at high redshift, demonstrating the essential property that CMB halo lensing can be applied over a very wide redshift range (well beyond the $z = 2$ limit of the figure). For PICO, the EB and TT estimators are roughly equivalent, offering important cross-validation of measurements because the systematics are very different for temperature and polarization.

This is illustrated in Fig. **??**, which shows the mass sensitivity of PICO using a spatial filter optimized for extracting the mass of halos (**?**). The curves give the one-sigma noise in a mass measurement through the filter as a function of redshift. Their flattening at high redshift reflects the fact that CMB lensing is sensitive over a broad range of redshifts, extending well beyond the limit of $z = 2$ of the figure. We see that PICO can measure the mass of individual low-mass clusters ($\sim 10^{14}\,M_\odot$) over a wide redshift range, and by stacking we can determine the mean mass of much smaller halos, including those hosting individual galaxies.

Halo lensing will enable use to calibrate the galaxy cluster mass scale critical for our cosmological analysis of PICO cluster counts, as mentioned above. It also gives us a unique tool for measuring the relation between galaxies and and their dark matter halos during the key epochs of cosmic star formation at $z \geq 2$, not reachable by other means. This will provide valuable insight into the role of environment on galaxy formation during the rise to and fall from the peak of cosmic star formation at $z \sim 2$. From a complementarity perspective, the high-resolution, high-frequency PICO channels will play an essential role in cleaning foregrounds for high-resolution ground-based halo lensing measurements at lower frequencies, particularly those derived from the temperature-based estimator, which is most contaminated by foregrounds.

• **Gravitational Lensing as Noise for Gravity Wave Science** does this belong here or in gravity waves? One of the most pronounced effects of lensing is the emergence of the 'lensing B-mode power spectrum', which is a result of gravitational lensing of E-modes into B-modes; see Figure **??**. reference figure in fundamental physics? When the tensor to scalar ratio $r \simeq 0.01$, the B-mode lensing power spectrum and the one from gravity waves have approximately the same level at $\ell = 80$, which is the angular scale at which the inflationary BB spectrum peaks. For lower levels

of r, this peak is masked by E-mode photons that are lensed into B. But the B-mode maps can be 'delensed' (**??**). The effect of lensing on E and B maps can be determined and undone if these maps are measured with few arcmin resolution and with sufficient depth. Forecasts for PICO show that at a minimum 73% of the lens-induced B-mode power will be removed for the baseline configuration, after accounting for foreground subtraction. 80% will be removed if the foregrounds do not degrade the inherent **SNR!**, rising to 85% for the CBE configuration. Without delensing PICO determination of r would be limited to $r >$??. We emphasize that PICO will be relying on its own data to conduct the delensing and foreground cleaning, thus avoiding reduced efficacy arising from the need to cross-calibrate experiments, identify common observing areas on the sky, not having frequency band coverage at the appropriate resolution to remove foregrounds, or from other systematic uncertainties.

• **Galaxy Formation via the Sunyaev-Zel'dovich (SZ) Effects** Not all CMB photons propagate through the universe freely; about 6% are Thomson-scattered by free electrons in the intergalactic medium (IGM) and intracluster medium (ICM). These scattering events leave a measurable imprint on CMB temperature fluctuations, which thereby contain a wealth of information about the growth of structures and the thermodynamic history of baryons. A fraction of these photons are responsible for the thermal and kinetic Sunyaev–Zel'dovich effects (tSZ and kSZ) (**??**). The amplitudes of the tSZ and kSZ signals are proportional to the integrated electron pressure and momentum along the line of sight, respectively. They thus contain information about the thermodynamic properties of the IGM and ICM, which are highly sensitive to astrophysical 'feedback'. Feedback is the process of energy injection into the IGM and ICM from accreting supermassive black holes, supernovae, stellar winds, and other sources. The tSZ effect will be used to measure ensemble statistics of galaxy clusters, which contain cosmological information, as well as to provide uniform cluster samples for galaxy formation studies in dense environments.

- Galaxy Clusters Galaxy clusters found via the tSZ effect provide a well-defined sample with a simple-to-model selection function. Sample of clusters such as these are straightforward to use for cosmological inference and studies of galaxy evolution in dense environments. The tSZ-selected sample from PICO will provide all clusters with masses above **double check** $\sim 3 \times 10^{14} M_{\odot}$ (defined with respect to the radius within which the average density reaches 200 times the critical) out to high redshifts, as long as the clusters have started to virialize. We forecast that PICO will find $\sim 1.5 \times 10^5$ total galaxy clusters, assuming the cosmological parameters from *Planck* primary anisotropies and applying a galaxy mask, using only 70% of the sky. With redshifts provided by optical surveys and infrared follow-up observations, the PICO tSZ-selected cluster sample will be an excellent cosmological probe, with mass calibration provided by CMB halo lensing described above and optical weak lensing for clusters with $z < 1.5$.

- Compton-y map and tSZ auto-power spectrum In addition to finding individual clusters, multifrequency CMB data also allow the reconstruction of full-sky maps of the thermal SZ signal (Compton-y maps) via foreground removal algorithms similar to those used to obtain cleaned maps of the CMB. With its extremely low noise and broad frequency coverage, PICO will yield a definitive Compton-y map over the full sky, with high S/N down to angular scales of a few arcminutes. We quantify this expectation by reconstructing the Compton-y field using the needlet internal linear combination (NILC) algorithm (**?**) applied to sky simulations generated with the *Planck* sky model, with maps at all PICO frequencies (with appropriate noise added). The error bars on the reconstructed tSZ power spectrum are shown in Fig. **??**, in comparison to current measurements. The total $S/N = 1270$ for the PICO CBE configuration, with the PICO baseline configuration only $\approx 10\%$ lower. This is nearly two orders of magntiude larger than the current S/N from *Planck*.

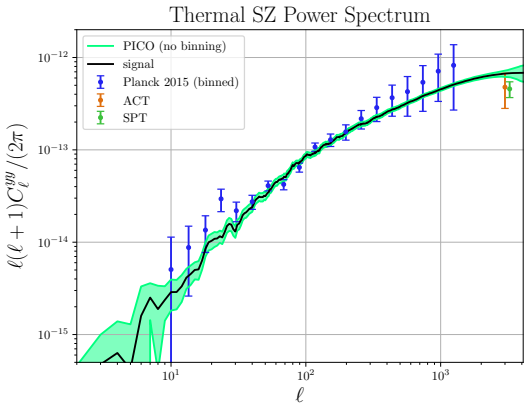

Figure 6: Constraints on the tSZ power spectrum from PICO and current data. The black curve shows the simulated tSZ power spectrum signal. The light green shaded region shows the error bars for PICO at each multipole, i.e., with no binning, as determined from NILC analysis of full-sky simulations. The blue points show the current constraints from Planck, which have been averaged into broad multipole bins. The orange and dark green points show the constraints from ACT and SPT, respectively, at a single multipole of $\ell = 3000$. The overall PICO $S/N = 1270$, nearly two orders of magnitude larger than current measurements.

Extremely strong constraints on models of astrophysical feedback will be obtained from the analysis of the PICO y-map, both from its auto-poewr spectrum and from cross-correlations with galaxy, group, cluster, and quasar samples. Like the CMB lensing map described above, the legacy value of the PICO y-map will be immense. As an example, we forecast the detection of cross-correlations between the PICO y-map and galaxy weak lensing maps constructed from LSST and WFIRST data. Considering the LSST "gold" sample with a source density of 26 galaxies/arcmin^2 covering 40% of the sky, we forecast a detection of the tSZ – weak lensing cross-correlation with S/N = 3000. At this immense significance, the signal can be broken down into dozens of tomographic redshift bins, yielding a precise breakdown of the evolution of thermal pressure over cosmic time. For PICO and WFIRST (assuming 45 galaxies/arcmin^2 covering 5.3% of the sky), we forecast S/N = 1100 for the tSZ – weak lensing cross-correlation. The WFIRST galaxy sample extends to higher redshift, and thus this high-S/N measurement will allow the evolution of the thermal gas pressure to be probed to $z \approx 2$ and beyond, the peak of the cosmic star formation history. These transformative measurements will revolutionize our understanding of galaxy formation and evolution by distinguishing between models of feedback energy injection at high significance. Additional cross-correlations of the PICO y-map with quasar samples, filament catalogs, and other large-scale structure tracers will further demonstrate its immense legacy value, providing valuable information on baryonic physics that is complementary to inferences from the lensing cross-correlations described earlier.